PHYSICAL REVIEW D

PARTICLES AND FIELDS

THIRD SERIES, VOL. 8, NO. 1 1 July 1973

Recoil-Proton Polarization in Neutral-Pion Photoproduction Between 1000 and 1800 MeV*

N. Tanaka,† M. M. Castro, R. H. Milburn, W. B. Richards,‡ J. P. Rutherfoord, and B. F. Stearns§
Department of Physics, Tufts University, Medford, Massachusetts 02155

M. Deutsch, P. M. Patel,‖ and K. Tsipis**
Laboratory of Nuclear Science and Department of Physics, Massachusetts Institute of Technology, Cambridge, Massachusetts 02139
(Received 27 December 1972)

Measurements are presented of the recoil-proton polarization for π^0 photoproduction angles near 64° in the c.m. system. The steep angular dependence observed by others at lower energies persists to at least 1500 MeV, and the polarization crosses through zero near 63° over the entire 900–1600-MeV energy interval. Summary fits are made to available recoil-proton polarization data, 950–1250 MeV, and are found to require terms of order $\cos^3\theta$, but no higher.

I. INTRODUCTION

We have measured the polarization of the recoil proton in neutral-pion photoproduction for incident photon energies between 1000 and 1800 MeV, at a mean pion production angle of 64.5° in the center-of-mass system. The experiment was performed at the Cambridge Electron Accelerator. Section II discusses the technique and the apparatus, Sec. III the data reduction procedure, Sec. IV the results, and Sec. V presents discussion and comparison with other experiments.

II. TECHNIQUE AND APPARATUS

Bremsstrahlung produced on an internal synchrotron target by an 1800-MeV electron beam passed through a collimator, sweeping magnets, and a scraper before striking a 5.08-cm liquid-hydrogen target (Fig. 1). Photons from the decay of the neutral pion passed through a permanent 700-g cm field into a shower detector consisting of a tantalum-plate optical spark chamber, a scintillation counter, and a lead-glass Čerenkov-counter hodoscope. Pulse heights from the scintillation counter and Čerenkov counters, together with hodoscope information, were recorded on film along with the shower-chamber pictures. The recoil proton entered a spectrometer consisting of a scintillation counter and two thin-plate optical spark chambers at each end of a dipole magnet providing mean deflection of 15°. This proton arm subtended 2.7×10^{-3} sr at the target and provided momentum resolution $\Delta p/p = 0.02$. Time of flight between the two scintillation counters and pulse-height information from the 2.5-cm-thick downstream counter permitted rejection of particles other than protons. The details of the proton spectrometer and the photon detection system are given in Ref. 1. The protons from the spectrometer entered a spark chamber built of aluminum-sheathed graphite plates, each 91.4 cm square and containing 1.27 cm of graphite, 0.05 cm of aluminum, and epoxy cement to total 1.40 cm. Sixty-one plates were mounted with 1.27 cm spacing in a gas-tight enclosure filled with helium at slightly above atmospheric pressure. Tests based upon minimum-ionizing cosmic radiation indicated that the chamber would have been only negligibly more sensitive were the expensive He-Ne mixture used instead of pure helium. The chamber was photographed in 90° stereo on 35-mm Linagraph Shellburst film

Copyright © 1973 by The American Physical Society.

through an optical system employing parabolic-cylindrical mirrors as field elements.

III. DATA REDUCTION

During the experimental runs about 160 000 events were photographed, after a coarse electronic selection based upon pulse heights in the Čerenkov and scintillation counters and time of flight in the spectrometer. The proton spectrometer and γ-spark chamber pictures were scanned and measured automatically on the MIT SPASS system.[2] About 25 percent of the events passed rigid requirements set to define neutral-pion photoproduction. Included in these events is a background of proton Compton scatterings estimated to be less than 7 percent over the photon energy range of interest. Also included are possible multipion productions. A Monte Carlo estimate placed this background at less than 3 percent of the accepted events.[3] Carbon-chamber photographs of the events selected by SPASS were then scanned and measured automatically by an early version of the SPASM system, then at Harvard,[4] and the various measurement data were merged onto a common set of computer tapes.

Polarization determinations are extraordinarily sensitive to small systematic errors in angular measurements. To assist in the reduction of the proton-carbon scattering data a set of grid lines intersecting on a 20-cm lattice were ruled on both carbon-plate spark-chamber windows and were photographed at the beginning and end of each roll of film. Separate photographs were made of wires stretched 61 cm in front of each of the windows to permit determination of the effective camera locations, in the two views, as a function of the chamber gap number, to allow for certain optical system distortions. Using averaged measurements of the photographed grids as made on a Vanguard film-plane digitizer, an optimized 22-coefficient function was calculated to map from the film plane onto the window grid of each view. Separate functions were determined for each 20-cm×20-cm square cell of the chamber window, and then the individual mappings were assembled into a continuous weighted average to eliminate discontinuities at the cell boundaries. The aim was to obtain a mapping that was conformal not only over large areas but also over the 15–20-cm regions that are critical for the determination of projected scattering angles of individual protons. The individual events as measured by the SPASM system were first mapped onto the film plane to correct for lens and CRT distortions, then onto the planes of the spark-chamber window grids, and then into real space, using a smoothed representation of the effective camera locations for each view. It is believed that this over-all procedure effectively compensated for both the intrinsic pin-cushion distortion of the parabolic field mirror system and the smaller scale distortions associated with the incidental bending of the large flat mirrors required to fit the optics onto the accelerator floor.

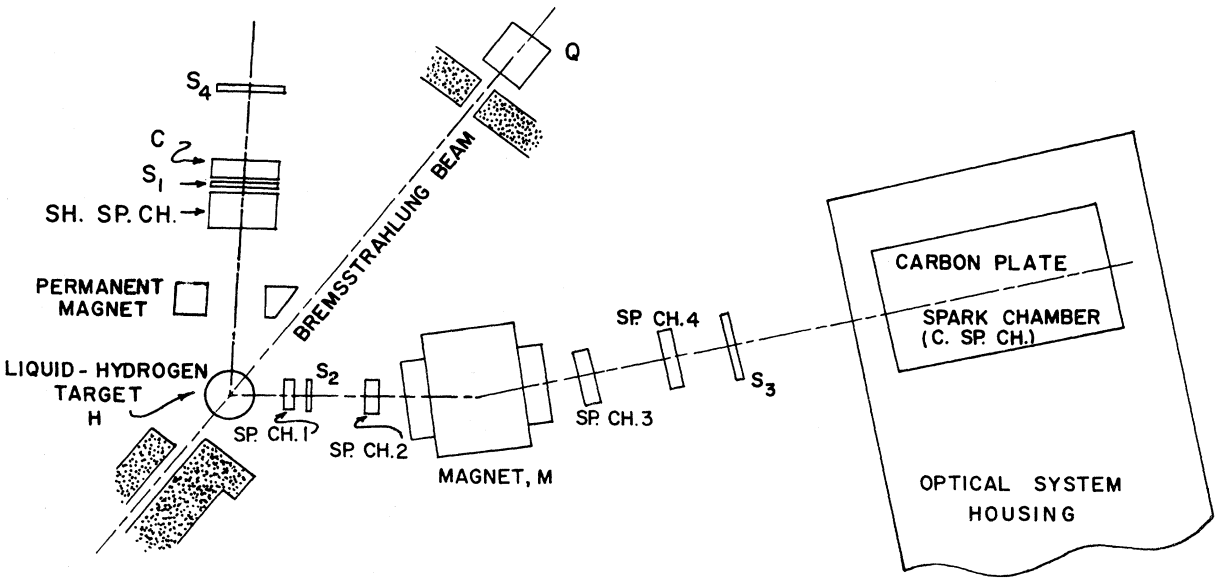

FIG. 1. Arrangement of experimental equipment.

The gross mapping fitted the 20-cm-cell vertices on the windows to ±0.06 cm, at worst. A check on a smaller geometrical scale was carried out using actual proton tracks as mapped by the above procedure. Measurements of two successive spark locations were used to predict the location of the spark preceding the pair for comparison with actual measurements of that spark. The precision of transverse measurement of individual spark positions was found to be ±0.1 cm in the top view (looking down on Fig. 1) and ±0.13 cm in the side view. The mean extrapolated spark location did not deviate from the expected straight line more than 0.010 cm in the top view and 0.015 cm in the side view.

For each event so measured and mapped scatterings were detected by dividing the spark trail into two portions and fitting a straight line in space to each portion, weighting the individual sparks to account for multiple Coulomb scattering appropriate to the scattering energy as inferred from the known incident energy and range of the particle. Such fits were obtained for all possible subdivisions of the track having at least two sparks in each of the two branches. The mean points of closest approach of the two fitted lines were determined and acceptable fits were required to have this point lie between the two assumed track segments. The closest approach distance, which was distributed with standard deviation 0.064 cm, was required to be less than 0.152 cm. A goodness-of-fit parameter was also calculated and, in case of ambiguities, the scattering was assumed to occur in the plate giving the best goodness of fit. No specific tests were made to detect double or plural scatters. For the selected fit the angles of scattering, the proton energy at scatter, and the inelasticity of the event were calculated. This last was determined from the incident momentum and measured range of the proton. This procedure yields "scatterings" down to angles of about 2°, below which the algorithm becomes progressively less reliable. Proton-carbon analyzing powers and an estimated uncertainty thereof were determined for the conditions of each scattering event using an extension of tables and a program prepared at the California Institute of Technology.[5] Data summary tapes were prepared and used to calculate the proton polarization and other results for a variety of cuts and conditions.[6] All data were subjected to cuts correlating a proton's trajectory in the spectrometer with its initial path in the carbon chamber in order to minimize spurious events.

Since it was known that a systematic angular error of as much as a few tenths of a degree could seriously affect the computed polarizations, an additional normalization procedure was carried out. For this, all events scattering at 2° or more, among which small-angle and other events of negligible analyzing power are vastly predominant, were assigned an analyzing power of 1.0 and the resulting spurious proton "polarization" was calculated for scatterings in each of the spark-chamber plates. For each plate an empirical redirection of the polar axis of scattering was effected to minimize a smoothed representation of these spurious "polarizations." For the chamber view relevant to the experiment—the top view—the spurious polarizations were approximately a constant 0.05 and were compensated by projected shifts of about 0.05° in the effective forward direction. The scattering angles for each event as renormalized in this way, together with the corresponding analyzing powers, were also recorded on the data summary tapes. A comparison of results calculated both from the original data and from this renormalization of them provides a measure of the residual systematic uncertainties in this experiment.

To confirm that the track-fitting routines selected legitimate p-carbon scatterings all data with measured inelasticity of scattering less than ±10 MeV (within the measurement resolution) were distributed in 1° laboratory scattering-angle bins between 6° and 20°, and in 20-MeV energy bins from 90 to 210 MeV, plus one bin extending to 300 MeV. For each bin an average elastic differential cross section was estimated from an interpolation of existing data.[5] The elastic scattering-angle distribution was predicted for each of 7 ranges of energy at scattering and was normalized to the number of scatterings in that range. The results were summed over the whole (90–300 MeV) energy range, to obtain adequate statistics, and the predicted occupancy of each 1° angular bin was compared with the observed numbers. Including all angles 7°–20° in 13 bins the observed numbers fitted to give a combined $\chi^2 = 4.35$ for 6 degrees of freedom, with a corresponding probability of 0.6. Between 6° and 7° an excess of events was observed, diminishing from a 100 percent excess below 150 MeV to about 50 percent at 300 MeV. These events are interpreted as coming from the tail of the multiple scattering distribution folded into our angular resolution. An additional comparison was made between the observed energy distribution and the suitably integrated cross-section estimates. Again, for 7°–20° and 90–300 MeV, the correspondence was satisfactory in terms of the known spectrum of incident protons corrected for inelastic scattering and absorption processes which may have occurred during passage through the spark chamber. The energy and angular range used in these tests contains the

predominant contributors to the effective proton-carbon analyzing power, and the above checks give us additional confidence that our procedures properly select and measure bona-fide proton-carbon scattering events.

IV. RESULTS

Our results are summarized in Fig. 2 in which proton polarizations as calculated from the *renormalized* angles are plotted against incident photon energy. Polarization +1 corresponds to a proton spin in the direction of $\vec{k}_\gamma \times \vec{q}_{\pi^0}$. Mean pion production angles are indicated. The error bars are statistical. The data include all p-carbon scattering angles above the angle max [7°, 10.9° − 0.0289T], where T is the laboratory kinetic energy at scattering, in MeV. This arbitrary cutoff eliminates potential dilution from multiple-scattering events but does not seriously affect the statistical accuracy of the polarization estimate. To illustrate the sensitivity of the data to various assumptions, there are marked against each error bar points corresponding to the following alternatives: (a) the use of all scattering angles greater than 3°; (b) the use of the original unnormalized scattering angles greater than 3°; (c) data in which an estimated uncertainty of the analyzing power data has been added to, or (d) subtracted from, that analyzing power, for all renormalized scattering angles greater than 3°. It is seen that the results are remarkably insensitive to these variations. One may infer that the dominant contribution to the asymmetry comes from the larger scattering angles where the analyzing power is both large and well known and in which the angular normalization is not critical. Dilution resulting from multiple Coulomb scattering does not appear to be significant, even in the data cut off at 3°. Regardless of the cutoff used the very small angle scatters contribute very little on account of the small associated analyzing power.

Spurious asymmetries could also be introduced were protons which scatter at large angles to leave the spark chamber, or were the chamber and measuring systems less sensitive to such protons. The former contingency was avoided by limiting measurements to tracks incident on the central portions of the spark chamber plates.

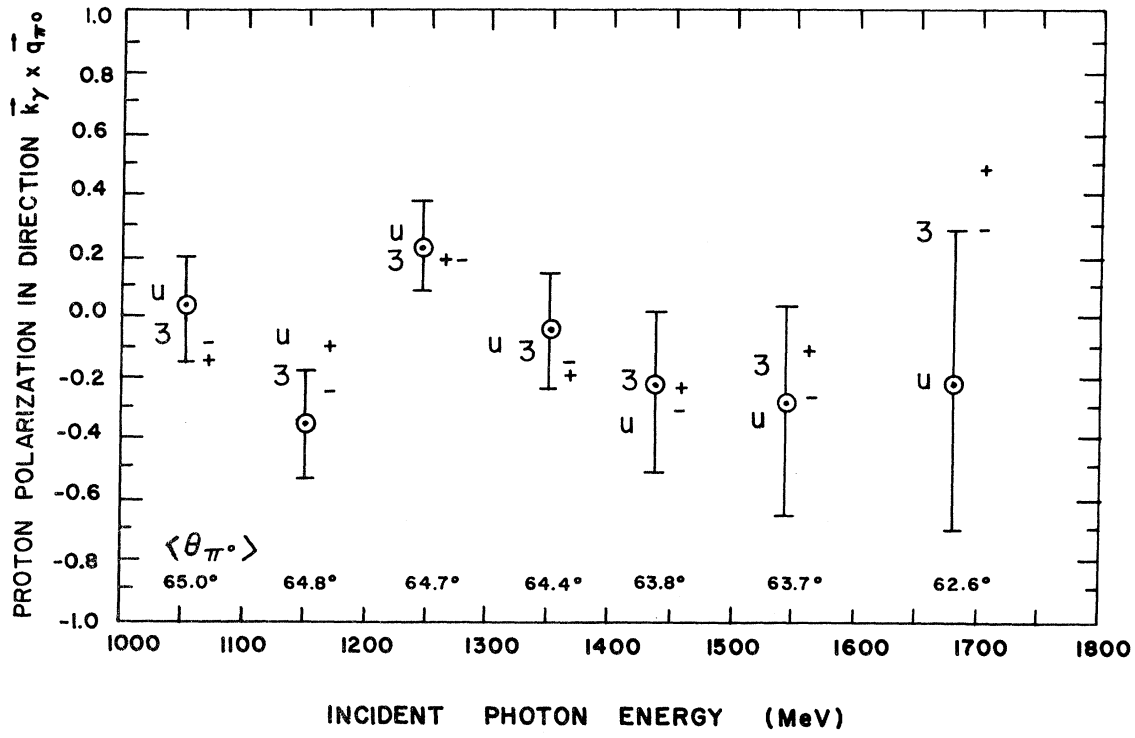

FIG. 2. Recoil-proton polarization near 64° pion production angle: results of this experiment. Points with indicated errors use renormalized p-carbon scattering angles cut off near 7° (see text). Also indicated are polarizations with scattering angles cut off at 3° using renormalized angles (symbol "3"); using unnormalized angles (symbol "*u*"); using renormalized angles and analyzing power data to which an uncertainty has been *added* (symbol "+") or from which it has been *subtracted* (symbol "−"). Actual mean production angles are shown.

Either process would be expected to affect primarily the larger p-carbon polar scattering angles, the range of which extended out to 30°. Our results, as described in subsequent paragraphs, were tested for such an effect by a recalculation in which scattering angles greater than 15° were excluded. The remaining events, amounting to a little more than half of our data, yielded polarization values consistent with those obtained using the full sample. No systematic trend was evident as a result of this cut.

A further systematic check was performed by selecting all events with p-carbon scattering angles between 2° and 3° and computing from them a spurious proton "polarization" in terms of unit analyzing power. This test would be expected to reveal measurement asymmetries which are imposed upon small-angle scatterings expected, *a priori*, to be symmetric. For the renormalized angles the mean "polarization" was consistent with 0 with $\chi^2 = 5$ for 7 degrees of freedom. The same data for the unrenormalized angles were consistent with 0 polarization with $\chi^2 = 9.8$. It is evident from these various checks and from Fig. 2 that such systematic variations as may have been introduced by optical distortions and mapping approximations lie well within our statistical uncertainties.

For the purposes of further analysis and comparison with other experiments we shall take as our final results the polarizations calculated from the normalized scattering angles and all data having a p-carbon scattering angle above max [7°, 10.9° − 0.0289T]. These results are presented in Table I, separated according to whether the pion production angle was larger or smaller than 64.5° in the center-of-mass system. Also given in Table I are the corresponding results from two different experiments at the California Institute of Technology covering overlapping energy and angular regions.[7,8] In this table our errors as presented are the statistical estimates which include, as we have indicated, the range of likely systematic uncertainties. The errors for the other experiments are as quoted by the respective authors.[7,8]

V. DISCUSSION AND COMPARISON WITH OTHER EXPERIMENTS

The polarizations in Table I show strong angular dependence. To compare these data it is convenient to plot them, for each 100-MeV energy bin, against the mean center-of-mass pion production angle. This is done in Fig. 3. Also shown are minimum-χ^2 straight-line fits made under the assumptions that all the data are statistically compatible and that the variation over the 10° range is approximately linear. We have fitted the proton polarization to a function $P = a + b(\theta - 62°)$, and entered the coefficients a and b also in Table I. These coefficients in effect summarize current experimental knowledge of the recoil-proton po-

TABLE I. Recoil-proton polarization in direction $\vec{k}_\gamma \times \vec{q}_{\pi^0}$.

Photon energy [a] (MeV)	This expt.		Caltech [b]		Caltech [c]		$P = a + b(\theta - 62°)$ [d]	
	62.6°	66.5°	57°	62°	60.7°	65.3°	a	b
950			0.17 (±0.21)	−0.15 (±0.18)	0.66 (±0.33)	−0.08 (±0.15)	0.040 (±0.098)	−0.043 (±0.032)
1050	0.44 (±0.28)	−0.23 (±0.22)	0.26 (±0.14)	−0.32 (±0.13)	0.05 (±0.12)	0.03 (±0.10)	0.017 (±0.057)	−0.030 (±0.019)
1150	−0.08 (±0.23)	−0.59 (±0.21)	0.04 (±0.15)	−0.14 (±0.15)	0.42 (±0.10)	−0.04 (±0.13)	0.065 (±0.059)	−0.057 (±0.021)
1250	0.54 (±0.22)	−0.02 (±0.21)	0.58 (±0.17)	0.01 (±0.18)	0.29 (±0.18)	0.32 (±0.33)	0.267 (±0.083)	−0.053 (±0.027)
1350	0.23 (±0.25)	−0.42 (±0.29)	0.70 (±0.24)	0.08 (±0.27)			0.15 (±0.13)	−0.114 (±0.039)
1450	0.25 (±0.31)	−1.00 (±0.41)	0.76 (±0.43)				0.07 (±0.21)	−0.194 (±0.066)
1550	−0.03 (±0.42)	−0.67 (±0.54)					−0.01 (±0.43)	−0.16 (±0.17)

[a] Geometrical center of 100-MeV bin.
[b] From Bloom *et al.* (Ref. 7).
[c] From Cheng (Ref. 8).
[d] Straight-line fits based on mean pion production angle for each datum.

larization from π^0 photoproduction near 60° from 900 to 1600 MeV. Most significant is the indication that the recoil-proton polarization passes through zero at 63.3°±1.6° center-of-mass pion angle over the entire 900–1600-MeV photon energy interval. This angle corresponds to a range of squared momentum transfers from $t=-0.320\pm0.015$ $(\mathrm{GeV}/c)^2$ at 950-MeV photon energy to $t=-0.600\pm0.028\,(\mathrm{GeV}/c)^2$ at 1550 MeV. The center-of-mass energy ranges between the D_{15} and F_{15} resonances near 1680 MeV and the F_{37} resonance at 1950 MeV. At 1250 MeV there is a suggestion in the a coefficient (Table I) of a 2–3-standard-deviation peak in the energy dependence of the polarization at 62°, corresponding to a momentum transfer of −0.45 $(\mathrm{GeV}/c)^2$. However, there is no clear evidence of any structure in polarization as a function of t extending above or below this particular s-channel energy of 1.8 GeV. Further, experiments at higher energy, where t-channel processes are presumed to dominate, show large negative polarizations in this t range, in contrast to the zero crossing found here.[9]

In view of the steep angular dependence of the polarization near 62° it is interesting to compare these results with data at larger pion production angles. Information is now available from Daresbury[10] and Bonn[11] up to photon energies of 1250 MeV. For purposes of comparison and interpretation it is conventient to calculate from all polarization data the reduced cross section

$$P' = [k P(\theta)\sigma(\theta)]/(q\sin\theta), \qquad (1)$$

where $\sigma(\theta)$ is the differential production cross section at angle θ, and k and q are the photon and pion center-of-mass momenta, respectively. The reduced cross section is equal to the interference term in the helicity amplitudes, $\mathrm{Im}(H_1H_3^*+H_2H_4^*)$,

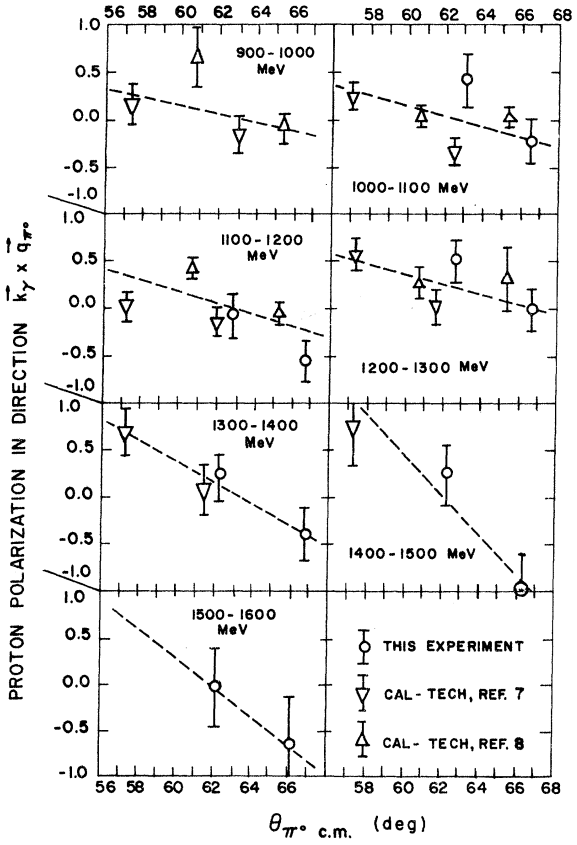

FIG. 3. Recoil-proton polarization dependence on pion production angle for different photon energies: data from this experiment and from earlier Caltech work near 60° (Refs. 7 and 8).

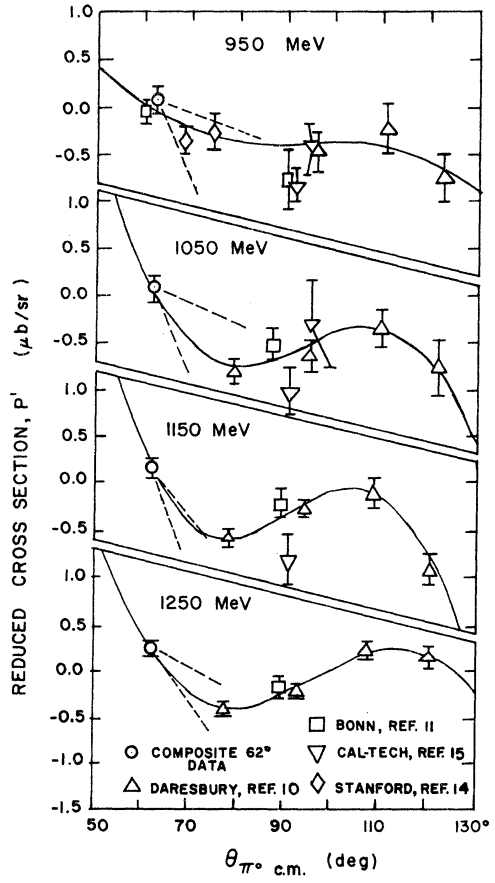

FIG. 4. Reduced cross section [cf. Eq. (1)] versus pion center-of-mass production angle for incident photon energies 950–1250 MeV: a summary of available data. The composite point at 62° and slope (dashed lines) are fitted to data from this experiment and from Caltech (Refs. 7 and 8). The solid curves are fits to the indicated points by the function $P'=A+B\cos\theta+C\cos^2\theta+D\cos^3\theta$ using the coefficients of Table II.

TABLE II. Expansion coefficients for the reduced cross section [Eq. (1)] in the form $P' = A + B\cos\theta + C\cos^2\theta + D\cos^3\theta$, where θ is the pion production angle in the center-of-mass system. [a]

E (MeV)	A (μb/sr)	B (μb/sr)	C (μb/sr)	D (μb/sr)
950	-0.397 ± 0.063	-0.03 ± 0.44	0.42 ± 0.53	2.4 ± 2.0
1050	-0.629 ± 0.077	-1.36 ± 0.57	1.67 ± 0.66	9.2 ± 2.8
1150	-0.361 ± 0.053	-1.86 ± 0.39	0.72 ± 0.46	11.8 ± 1.9
1250	-0.269 ± 0.038	-1.42 ± 0.27	2.25 ± 0.34	6.6 ± 1.3

[a] Utilizing data from Ref. 7, Ref. 8, Ref. 10, Ref. 11, Ref. 14, and the present experiment.

divided by[12] $\sin\theta$. Differential cross sections were interpolated where available from recent Daresbury work.[13] Reduced cross sections are plotted in Fig. 4, which summarizes currently available data above 900 MeV.[14,15] At 62° a composite point is entered representing a straight-line fit to the reduced cross sections obtained from the data of the present experiment and from the 60-degree Caltech experiments. The individual data points are treated as in Table I. Also indicated by dashed lines are the uncertainty ranges of the slopes of the straight-line fits associated with the 62° composite point. We have fitted these reduced cross sections to polynomials in $\cos\theta$, $P' = A + B\cos\theta + C\cos^2\theta + D\cos^3\theta$, which are also plotted in Fig. 4, using coefficients given in Table II. The third-degree term is indispensible for fitting the data near 60°, but higher terms are unnecessary. It is to be observed that the slope of the fitted curve at 62° lies within the uncertainty limits of the slope associated with the fit to the 60-degree data alone. The latter slope as measured in the present experiment remains approximately constant at $dP'/d\theta = -0.067 \pm 0.012$ μb/sr deg between 900 and 1500 MeV and is consistent with the same value up to 1600-MeV photon energy.

A full interpretation of all these data can, of course, only be made in the context of an overall analysis of pion photoproduction phenomena such as that of Walker.[12] On the other hand, it is difficult to imagine how our principal result—the apparent zero in the recoil-proton polarization at 62°–63° all the way from 900 to 1600 MeV—could arise from a complicated conspiracy of many contributing and resonating amplitudes. Neither would such a zero appear to be a reflection of a simple t-channel process, since θ_s, rather than t, determines its location over the whole range of s. The simplest *a priori* interpretation would be in terms of a weakly energy-dependent and real background amplitude which vanishes near 63° and against which imaginary resonant amplitudes interfere to produce the energy-dependent polarizations at larger angles. Presently available cross-section data are insufficient to resolve these speculations, although there appears to be a broad minimum in the differential cross section in the region 70°–90° in the c.m. system and 900–1300 MeV,[13] which suggests the vanishing of a significantly contributing amplitude.

ACKNOWLEDGMENTS

We wish to thank C. Bemporad, J. R. Sauer, C. K. Sinclair, K. Sisterson, and the staff and Director of the Cambridge Electron Accelerator for their important assistance during various phases of this experiment.

*Research supported by the U. S. Atomic Energy Commission under Contract No. AT(11-1)3023.

†Present Address: Los Alamos Scientific Laboratory, Los Alamos, N. M. 87544.

‡Present Address: Department of Physics, Oberlin College, Oberlin, Ohio 44074.

§Present Address: Department of Physics, Hobart and William Smith College, Geneva, N. Y. 14456.

‖Present Address: Department of Physics, McGill University, Montreal, Quebec.

**Present Address: Department of Biophysics, Massachusetts Institute of Technology, Cambridge, Mass. 02139.

[1] D. F. Jacobs, Ph.D. Thesis, Massachusetts Institute of Technology, 1970 (unpublished). See also Ref. 3 below.

[2] M. Deutsch, IEEE Trans. Nucl. Sci. NS-12, 69 (1965).

[3] N. Tanaka, Ph.D. Thesis, Tufts University, 1969 (unpublished), p. 131.

[4] C. A. Bordner, Jr., A. E. Brenner, and P. deBruyne, Radio Electron. Eng. 33, 171 (1967); A. E. Brenner, IEEE Trans. Nucl. Sci. NS-12, 241 (1965).

[5] C. S. Kretschmar, M. S. Thesis, Tufts University, 1969 (unpublished); W. A. McNeely, California Institute of Technology Internal Report No. 30, 1967 (unpublished).

Dependence upon a limited common pool of polarization data from p-carbon scattering is intrinsic to experiments using this reaction as an analyzer. The data relevant to the present experiment are from sources referenced in McNeely's report above. Kretschmar associated with each interpolated p-carbon analyzing power determination a quantitative uncertainty which reflected the statistical accuracy and interconsistency of the contributing measurements. The small ultimate effect of these uncertainties is discussed in Sec. IV, above, and is illustrated in Fig. 2. These tests do not rule out the possibility that the original results on p-carbon scattering may simply be wrong. This contingency would have a more severe effect on experiments in which large proton polarizations are observed than on the present one which demonstrates an apparent zero-crossing.

[6]Polarizations were obtained by maximizing the likelihood function

$$\mathfrak{L}(P) = \prod_i [1 + A(T_i, \theta_i, \Delta T_i) P \cos\varphi_i],$$

where φ_i is the azimuthal p-carbon scattering angle for each event and A is the corresponding analyzing power as a function of energy, polar angle, and inelasticity.

[7]E. D. Bloom, C. A. Heusch, C. Y. Prescott, and L. S. Rochester, Phys. Rev. Lett. 19, 671 (1967); E. D. Bloom, Ph.D. Thesis, California Institute of Technology, 1967 (unpublished), Table IV, p. 39.

[8]S. Cheng, Ph.D. Thesis, California Institute of Technology, 1970 (unpublished), Table 4.3, p. 69.

[9]M. Deutsch, L. Golub, P. Kijewski, D. Potter, D. J. Quinn, and J. Rutherfoord, Phys. Rev. Lett. 29, 1752 (1972); 30, 249(E) (1973).

[10]M. N. Prentice *et al.*, Nucl. Phys. B41, 353 (1972).

[11]P. Blüm *et al.*, Universität Bonn Physikalisches Institut Report No. PI-1-105, 1970 (unpublished).

[12]R. L. Walker, Phys. Rev. 182, 1729 (1969). (For definitions of $H_1, \ldots, H_4$.)

[13]P. S. L. Booth *et al.*, Daresbury Nuclear Physics Laboratory Report No. DNPL/P-95, 1971 (unpublished); also P. Spillantini and V. Valente, CERN Report No. CERN-HERA 70-1, 1970 (unpublished).

[14]D. E. Lundquist *et al.*, Phys. Rev. 168, 1527 (1968).

[15]Reference 8, page 69.

PHYSICAL REVIEW D VOLUME 8, NUMBER 1 1 JULY 1973

Cosmic-Ray Muon Integral Intensity Measurement Under Water*

Howard F. Davis
Department of Physics, Oregon State University, Corvallis, Oregon 97331

John G. Learned†
Department of Physics, University of Washington, Seattle, Washington

(Received 14 August 1972)

The cosmic-ray muon integral intensity ($E_{\mu\text{-threshold}} \gtrsim 1$ GeV/c) was measured under water with a detector of small angular aperture (6.5° full width at half maximum). The motivation of the work was to check the range-energy relation for muons under a medium, water, whose properties are very well known and whose atomic properties (Z, Z^2/A) are significantly different from "rock" used in underground measurements. The ratio of these measured relative muon intensities, converted to equivalent depths of standard rock, to those measured under rock and converted to standard rock, for 50 hg cm$^{-2} \lesssim d \lesssim$ 1000 hg cm^{-2} of equivalent standard rock, is 1.09± 0.06. This measurement shows that the range-energy interactions of muons are consistent between "rock" and water for $E_\mu \lesssim 240$ GeV.

I. INTRODUCTION

This experiment measured the relative integral intensity of single cosmic-ray muons with a small-angle aperture (the angle for full width at half maximum is $\theta_{\text{FWHM}} = 6.5°$) for water depths of 244 m and for slant-angle (zenith) detector orientations up to 75°. The purpose of this experiment was to establish accurately the consistency between muon range-energy interactions in water and rock.[1-3] The significant differences between water and "standard rock" are partially reflected in their atomic properties (Z/A, Z^2/A) and their specific densities [$(0.50, 3.67)_W$, $(0.50, 5.5)_R$, $(1.0)_W$, $(2.65)_R$].

A simple two-element small-angle-aperture detector telescope was constructed and used as the principal detector after a series of different configurations, generally of wider angular aperture, were experimented with in an early phase of the work.[4] Relatively hard muons, $E_\mu \gtrsim 1$ GeV, were necessary to trigger an event in the telescope. This directionally sensitive telescope registered the number of muons, in fixed time periods,